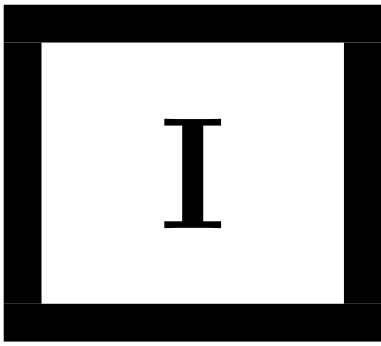

Publication I

J. Oksanen and J. Tulkki, *Linewidth enhancement factor and chirp in quantum dot lasers*, Journal of Applied Physics **94**, pp. 1983-1989 (2003).

Linewidth enhancement factor and chirp in quantum dot lasers

Jani Oksanen[a] and Jukka Tulkki
Department of Electrical and Communications Engineering, Helsinki University of Technology, Finland

(Received 10 February 2003; accepted 21 May 2003)

We have made a comparative study of the linewidth enhancement factor (LEF) and chirp in quantum dot (QDL's) and quantum well lasers (QWL's). The simulations are based on the quasiequilibrium approximation and on semiempirical transition energies and amplitudes of InGaAs quantum pyramid structures. We have accounted for the carriers confined in the active material as well as for the carriers in all the other material layers. It is found that in the quasiequilibrium approximation inhomogeneous broadening leads to asymmetric population of the quantum dot ground state. If the QDL is operated at the gain maximum, the asymmetry leads to nonzero chirp even for a single bound resonance state located at a large distance from other resonances. Our calculations show that, by detuning the laser emission to ~ 15 nm shorter wavelengths with a frequency selective cavity and by tailoring the resonance energies and inhomogeneous broadening, the LEF and chirp of a QDL can be made very small. This detuning does not add a substantial penalty to the efficiency of the laser. For QWL's, a similar reduction of chirp is generally not feasible due to the fundamentally different density of states. Therefore QDL's have an important advantage over QWL's as directly modulated light sources in applications where the stability of the emission wavelength is critical.
 [DOI: 10.1063/1.1591059]

I. INTRODUCTION

Quantum dot lasers (QDL's) are expected to have superior operational characteristics since the δ-function-like density of states (DOS) of the lasing material can be made to match the photon modes of the Fabry-Pérot cavity. This would give QDL's the maximum possible material gain for a given carrier density. In actual QD laser structures, however, the performance is limited by inhomogeneous broadening and by other nonidealities and losses. Recently it has been shown that the performance of QDL's is not limited by slow carrier relaxation (''phonon bottleneck'') since under lasing conditions the carrier dynamics is dominated by fast carrier-carrier (Coulomb) interactions.[1–3] Progress has also been made in reducing the inhomogeneous broadening and a very low threshold current and other nearly ideal operational characteristics have been demonstrated for QDL's.[4–7]

In a recent measurement, Saito *et al.*[4] showed that the chirp can be very low in QDL's. In their measurements, for a strong modulation of 1 GHz, the chirp was lower than 0.01 nm (2 GHz), an order of magnitude smaller than in the similar conventional quantum well laser (QWL) they used as a reference. Chirp causes problems in the channel selectivity of dense wavelength division multiplexing networks. Therefore low chirp would give QDL's an important advantage as light sources in high-capacity optical communications. Understanding how chirp depends on the lasing material and the structure parameters of the lasers has great technological significance.

In this work, we have studied theoretically the chirp in a QD laser similar to the one used in Ref. 4. In Sec. II we present the theoretical model used in the calculations. Section III describes the laser structures involved in the calculations, and Sec. IV presents the results. A short summary of the main results is given in Sec. V. In the Appendix we calculate the linewidth enhancement factor (LEF) for an isolated inhomogeneous QD ground state and show that it does not approach zero even at the limit of vanishing inhomogeneous broadening.

II. THEORY

The potential benefits of using QD's as the active material in semiconductor lasers were realized before the first QD lasers were fabricated. The advantage of the QDL regarding the temperature dependence of the threshold current was predicted theoretically by Arakawa and Sakaki in 1982.[8] They also reported experimental evidence of the reduced temperature dependence of the threshold current of QWL's set in a strong external magnetic field. The dependence of the gain and the threshold current on the size of quantum dots and their density in the lasing material was studied by Asada *et al.* in 1986.[9] The need to reduce the inhomogeneous broadening for maximization of the gain was pointed out by Vahala in 1988.[10] The gain and dynamical properties of QDL's based on InGaAs/GaAs were studied by Grundmann and Bimberg[11] and Bimberg *et al.*[12] According to the last reference the chirp of a QDL is zero for a single isolated emission line. Very recently, Schneider *et al.*[13] have studied the influence of electron-hole polarization on the dynamics of QDL's. They report substantial shift in the gain spectrum as a result of the coupling between the carriers in the wetting layer and the carriers that are relaxed in the dot states.

In this work we have made a comparative study of how the LEF and chirp depend on the change in the density of states when one goes over from conventional QWL's to

[a]Electronic mail: jani.oksanen@lce.hut.fi

InGaAs/GaAs QDL's. Our calculation focuses on a comparative study of the QD and QW lasers. Therefore we use the parabolic band model as a first order approximation. In addition, we study qualitatively the dependence of the LEF and the chirp on the carrier density and the energies of the bound QD states. We discuss the influence of many-particle effects briefly in the Conclusions.

In the linear approximation the material gain is given by[12]

$$G_m(\omega, \mathbf{u}_A) = \frac{\pi e^2 m_0^{-2}}{\varepsilon_0 c_0 n_r \omega} \sum_{m,n,\beta} \int dk\, g(k) |\mathbf{p}_{if}^{mn\beta \mathbf{u}_A}|^2 \times L(E_{cv}(k) - \hbar\omega)[f_c(k) - f_v(k)], \quad (1)$$

where ω is the angular frequency of the photon, $\mathbf{u}_A$ the unit vector along the polarization of the photon, and n_r the refractive index of the material. The DOS (spin degeneracy included) is denoted by $g(k)$ and the function L describes the spectral linewidth broadening. In the argument of L, $E_{cv}(k)$ is the direct transition energy from conduction to the valence band. In Eq. (1) $\mathbf{p}_{if}^{mn\beta \mathbf{u}_A}$ is the momentum matrix element evaluated for the photons with polarization along the unit vector $\mathbf{u}_A$. The functions $f_{c,v}$ denote the quasi-Fermi functions for the conduction and valence band electrons, respectively. The sum is taken over the different subbands of the structure: m stands for the electron subbands, n for the hole subbands, and β indicates the different (heavy and light) hole (HH and LH) bands. The integration is over the electron wave vector k.

The conventional Lorentzian linewidth broadening function becomes inaccurate below the band gap energy. Therefore we have used the broadening factor suggested by Asada[14]:

$$L(\hbar\omega - E_{cv}) = \frac{[\Gamma / f_v(0)] f_v(\hbar\omega - E_{cv})}{(\hbar\omega - E_{cv})^2 + \{[\Gamma / f_v(0)] f_v(\hbar\omega - E_{cv})\}^2}. \quad (2)$$

Here $\Gamma = \hbar/\tau$ is the lifetime broadening factor. Equation (2) resembles a Lorentzian except for the lower part of the spectrum, where it decays exponentially. The exponential decay (included in the Fermi factors) results from additional broadening effects caused by intraband relaxation processes.[14] Without this exponential decay the absorption of the bulk layers even below the band gap could dominate over the modal gain of the QD's.

The dependence of the momentum matrix element on the direction of the electron wave vector in the well layers has been taken into account by the approximate formula[15]

$$|\mathbf{p}_{if}^{mn\beta \mathbf{u}_A}|^2 = \begin{cases} \frac{1}{4}(1 + \cos^2\theta) m_0 E_p/2, & \text{TE, } \beta = \text{HH}, \\ \frac{1}{2}\sin^2(\theta) m_0 E_p/2, & \text{TM, } \beta = \text{HH}, \\ \frac{2}{3} - |\mathbf{p}_{if}^{mnHH \mathbf{u}_A}|^2, & \beta = \text{LH}, \end{cases} \quad (3)$$

where $\cos^2\theta = [E_c^m(0) + E_v^{n\beta}(0)]/[E_{cv}(k) - E_g]$. $E_c^m(k)$ $[E_v^{n\beta}(k)]$ denotes the energy of the electron (hole) measured from the conduction (valence) band edge, $E_{cv}(k)$ is the total transition energy, and E_g is the band gap energy of the QW material. In Eq. (3) E_p is the Kane matrix element.

The average material gain of the mainly inhomogeneously broadened QD layer is obtained statistically from Eq. (1) and given by[11]

$$G_{\text{QD}}(\omega, \mathbf{u}_A) = \frac{2\pi e^2 m_0^{-2}}{\varepsilon_0 c n_r \omega V} \sum_{m,n,\beta} P(\hbar\omega, \sigma) \times |\mathbf{p}_{if}^{mn\beta \mathbf{u}_A}|^2 [f_c(E_c) - f_v(E_v)]. \quad (4)$$

The inhomogeneous broadening function of the QD energy levels, $P(\hbar\omega, \sigma)$, is assumed to be Gaussian:

$$P(\hbar\omega, \sigma) = \frac{1}{\sqrt{2\pi}\sigma} \exp\{-[\hbar\omega - E_{cv}(k)]^2/(2\sigma^2)\}. \quad (5)$$

To account for the lower maximum gain of strongly broadened QD states, the standard deviations in Eq. (5) were calculated using the relative standard deviation σ_r and the relation $\sigma = \sigma_r[E_c^m(0) + E_v^{n\beta}(0)]$ [see Eq. (3) for the symbols].

In addition to the carriers confined in the QD's, we account for the carriers in the wetting layer and the barrier and optical cladding layers, whose material gain is calculated using Eq. (1). The total gain G is the sum of all these material gains weighted by the appropriate optical confinement factors.

According to the Kramers-Kronig relation the refractive index n_r and the gain are related by[16]

$$n_r(\hbar\omega) - 1 = \frac{ch}{2\pi^2} P \int_0^\infty \frac{-G(E)}{E^2 - (\hbar\omega)^2} dE. \quad (6)$$

For the calculation of the change of n_r, the numerical integration can be limited to that part of the spectrum where the gain changes as a result of a change in the carrier density. The upper limit of integration is set to several hundreds of meV above the band gap of the optical cladding layer and the lower limit is below the broadened QD ground state spectrum.

The linewidth enhancement factor was calculated from[16]

$$\text{LEF}(\hbar\omega) = -2k_0 \frac{\partial n_r / \partial n_e}{\partial G / \partial n_e}, \quad (7)$$

where k_0 is the photon wave number in vacuum and n_e is the carrier density.

In the first approximation the chirp of the laser can be calculated using the standard laser rate equations

$$\frac{dN}{dt} = \frac{I}{e} - v G(N) S - \frac{N}{\tau_{\text{rec}}}, \quad (8)$$

$$\frac{dS}{dt} = v(G(N) - \alpha) S + \frac{N\eta}{\tau_r}, \quad (9)$$

where N is the number of electrons in the system, I the injection current, v the velocity of light, S the number of photons in the cavity, and τ_{rec} the recombination lifetime of the carriers with the stimulated emission excluded. The total losses are denoted by α, the radiative carrier lifetime by τ_r, and the coupling of spontaneous emission to the laser mode

by η. Solving Eqs. (8) and (9) gives the carrier density during the relaxation oscillations caused by direct current modulation. Knowing the carrier density as a function of time enables us to determine the corresponding changes in the refractive index. The chirp is then obtained from $\Delta\lambda = (n_r^{\max} - n_r^{\min})\lambda_0$, where $n_r^{\max}$ and $n_r^{\min}$ are the maximum and minimum values of n_r experienced during the relaxation oscillations.

The rate equation model in Eqs. (8) and (9) assumes single mode operation of the laser and neglects a number of unidealities like the spectral and spatial hole burning effects and carrier diffusion processes. These processes will be the subject of a separate work.

III. SIMULATED STRUCTURES

The QDL structure selected for simulation mimics the QDL used in Ref. 4. It includes a 1.5 μm $n-Al_{0.3}Ga_{0.7}As$ optical cladding layer, a 50 nm GaAs barrier layer, three InAs QD layers separated by 55 nm GaAs barrier layers, again a 50 nm GaAs barrier layer, and a 1.5 μm $p-Al_{0.3}Ga_{0.7}As$ cladding layer. We also included three 1 nm thick wetting layers giving rise to one bound state of electrons and holes each. The two-dimensional density of the quantum dots is $5.7\times10^{10}\,\mathrm{cm}^{-2}$. The laser cavity has a highly reflective coating to give a reflection coefficient of $R=0.99$, its length is 970 μm, and its width is 2.5 μm.

A quantitatively accurate calculation of the electron and hole confinement energies in a QD is difficult due to the large uncertainties in the shape and dimension of the quantum dots in the fabricated QD's. Therefore we used three semiempirical sets of QD electron and hole confinement energies in our calculations. The first set of energy levels (ES1) is shown in the inset of Fig. 1 and the other two (ES2 and ES3) in Fig. 2. Comparing calculated LEF and chirp values for the three sets of QD energy levels should give a good qualitative picture of how the dynamical properties of the QDL change as a function of the strength of the confinement effect. The results shown in Figs 1, 3, and 4(a)–4(c) correspond to ES1. For ES2 and ES3 we only give a summary of the results in Sec. IV. For all these structures the relative standard deviation of inhomogeneous broadening was set to $\sigma_r=0.12$, resulting in ground state full widths at half maximum (FWHM's) of 20 meV for ES1 and ES2 and 40 meV for ES3.

The oscillator strength involved in the expressions for gain [Eqs. (1) and (4)] depends critically on the overlap integrals of the envelope wave functions. Recently it has been shown that the envelope overlap factors of the ground state transitions can be as low as $|\langle\Psi_0^c|\Psi_0^v\rangle|^2\approx0.17$ for small pyramidal QD's.[17] Here we used $|\langle\Psi_0^c|\Psi_0^v\rangle|^2$ as a parameter and studied its influence on the LEF and the chirp. The results shown in Figs. 1–4(c) were obtained with $|\langle\Psi_0^c|\Psi_0^v\rangle|^2=0.5$. For the bound QD states we assumed the degeneracy factor $g_{np}=2n_p$ where $n_p=1,\ldots$ is the principal quantum number.

An ideal reference QW laser would be based on exactly the same III-V compounds as the QDL above and have the same emission wavelength of 1.24 μm. However, a GaAs/InGaAs QW structure is limited to shorter wavelengths. Therefore we used a multiple-QW laser made of the quaternary compound $Ga_xIn_{1-x}As_yP_{1-y}$ as a reference. The Ga and As fractions were set to $x=0.26$ and $y=0.56$ in the well (well width 7.2 nm) and $x=0.15$ and $y=0.33$ in the barrier (barrier width 10 nm). This QWL has approximately the same emission wavelength as the QDL structures above.[18] The calculation of the QWL gain is based on the parabolic approximation, accounting for one confined electron level and three confined hole levels as well as the three-

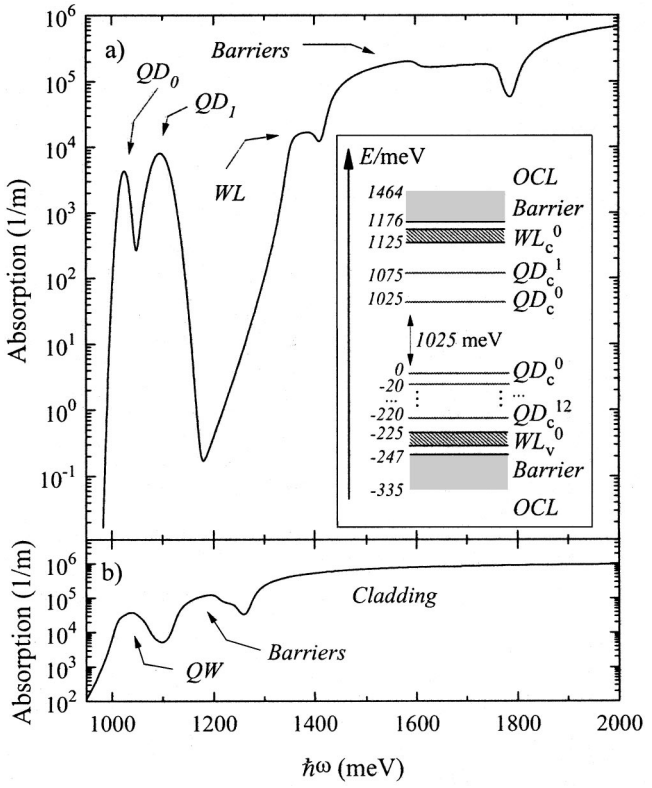

FIG. 1. The absorption spectra of the laser structures for very low carrier densities: (a) the quantum dot laser (ES1) and (b) the quantum well laser. The inset in (a) shows the energy levels of ES1.

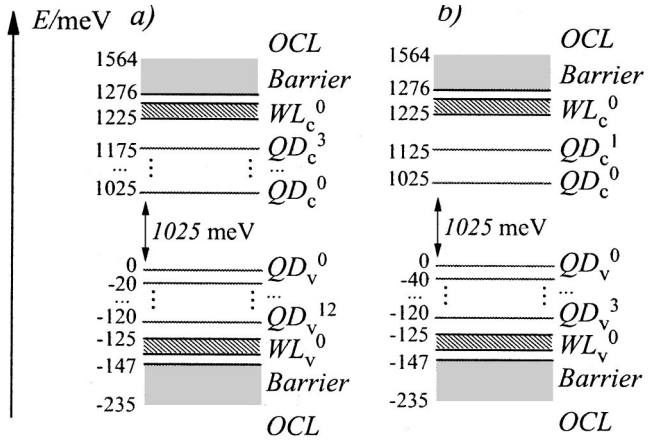

FIG. 2. The other choices of energy levels (not in scale) used in the calculations: (a) ES2 with four conduction band energy levels and (b) ES3 with two widely separated conduction band energy levels.

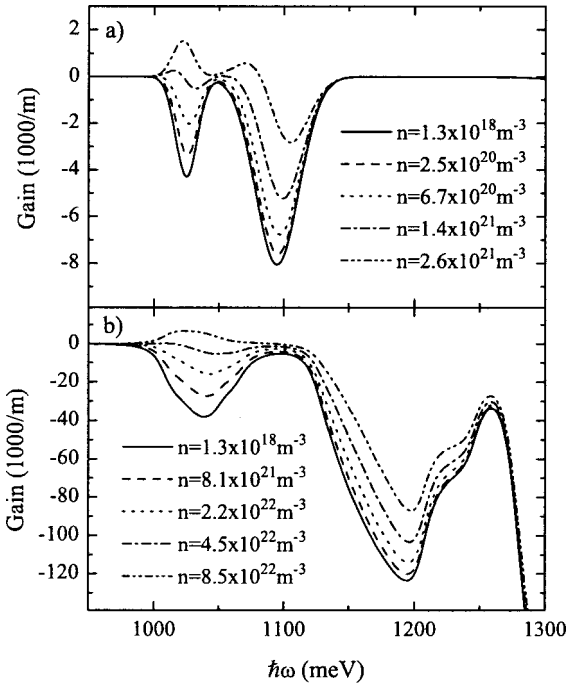

FIG. 3. (a) QDL gain for selected carrier densities in the vicinity of the lowest recombination lines QD_0 and QD_1 of ES1 and (b) QWL gain for the same photon energy range.

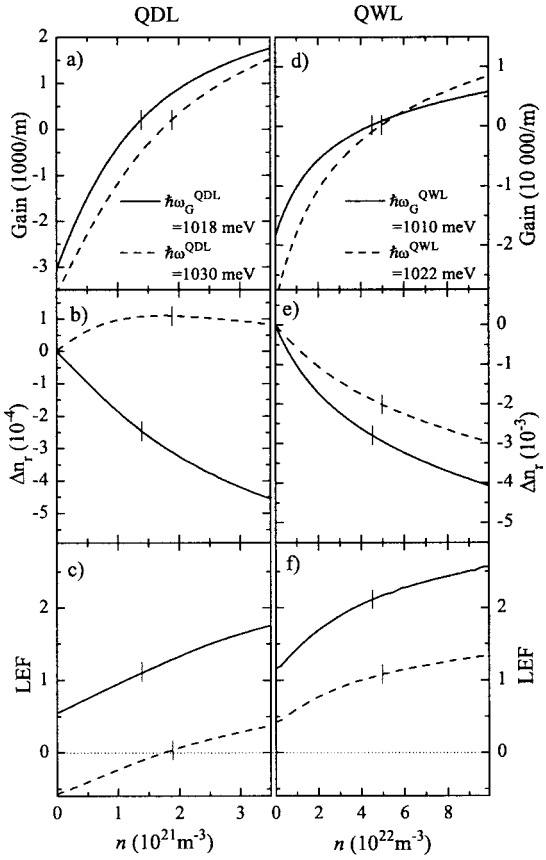

FIG. 4. The gain of (a) the QDL and (d) the QWL, the change of the refractive index of (b) the QDL and (e) the QWL, and the LEF as a function of carrier density for (c) the QDL and (f) the QWL. Photon energies $\hbar\omega_G$ (solid lines) correspond to the energies of the gain maximum at lasing conditions ($\alpha=210$/m) and $\hbar\omega$ (dashed lines) energies slightly above the gain maximum to demonstrate the reduction of LEF due to laser detuning. The short vertical lines denote the threshold carrier densities for total losses of 210/m.

dimensional (3D) continua corresponding to the barriers and the cladding.

IV. RESULTS AND DISCUSSION

The results were calculated for the transverse electric (TE) mode and room temperature with linear polarization fixed in the QW plane. Figure 1 shows the absorption spectra for the QDL and QWL structures. The intrinsic lifetime used for calculations of the lifetime broadening in the QW's was set to $\tau=70$ fs.[15] The gain spectra in the vicinity of the QD and QW emission lines for different carrier densities are shown in Fig. 3.

Figure 4 shows the calculated gain, change of the refractive index relative to zero injection level, and LEF of the QDL and QWL as a function of the carrier density for two different transition energies, specified in detail below.

A. Laser operation at the gain maximum

The total losses and the frequency response of the laser cavity determine the steady state operating point of the laser. For a 30 μm wide QDL an internal loss of 130/m has been reported.[6,19] In determining the operating point of the simulated laser structures we used a slightly larger, but still very small, value of 210/m for the losses. Assuming that there is no frequency selection (except for the Fabry-Pérot mode structure) by the cavity, we obtain for ES1 and the QWL the threshold carrier densities $n_{\mathrm{th}}^{\mathrm{QDL}}=1.4\times10^{21}\,\mathrm{m}^{-3}$ and $n_{\mathrm{th}}^{\mathrm{QWL}}=4.5\times10^{22}\,\mathrm{m}^{-3}$. The maximum values of gain ($G=210$/m) for these carrier densities are located at emission energies $\hbar\omega_G^{\mathrm{QDL}}=1018$ meV and $\hbar\omega_G^{\mathrm{QWL}}=1010$ meV.

Comparing the energy of the QDL gain maximum with the resonance energy of 1025 meV, we conclude that for the given value of $n_{\mathrm{th}}^{\mathrm{QDL}}$ *the gain maximum of the QDL does not coincide with the (joint) DOS maximum* but is redshifted from the maximum of the QDL ground state DOS by 7 meV. Similar redshifts of gain maxima were obtained for other choices of energy levels. The redshift of the gain maximum from the DOS maximum is a general result for inhomogeneously broadened QD ensembles obeying Fermi-Dirac statistics. This implies that at finite temperature the ground state gain of a QDL is not symmetric with respect to the gain maximum (see Fig. 3) and accordingly the LEF of a QDL is never zero at this operation point. For reference, we have shown in the Appendix that this result holds true even when the influence of the higher QD emission lines and the wetting layers is neglected.

The LEF value 1.1 obtained for ES1 is lower than the LEF value 2.2 of the reference QWL only by a factor of 2 [see Figs. 4(c) and 4(f)]. In the case of the QDL it is noted that for ES1 only one-third of the total LEF value is due to the excited states, leaving a contribution of 0.7 to arise from the ground state alone.

It is reasonable to expect that the LEF decreases when the inhomogeneous broadening σ of the ground state decreases. This was confirmed by our calculations. With the

inhomogeneous broadening reduced from FWHM=20 to 10 and 5 meV, the LEF is reduced from 1.1 to about 0.9 and 0.7, respectively. However, it was found that the LEF does not go to zero even in the limit FWHM$\rightarrow$0.

The calculations were repeated for other choices of energy levels. For ES3 we obtained LEF=1.3. The larger value of LEF (compared to ES1) is due to the larger inhomogeneous broadening of the ground state: the gain peak is now located at a lower energy (further away from the DOS maximum) and the ground state contribution to the LEF has increased. In contrast to ES1 and ES3, the LEF for ES2 is only slightly lower (LEF$\approx$1.8) than for the QWL (LEF$\approx$2.2), because the gain spectrum does not have as clear a gap between the first excited level and the wetting layer.

We also studied the effect of the total cavity losses and the overlap integral of the dipole amplitude on the LEF for ES1. The minimum LEF of about 0.8 was obtained for total losses of about 2000/m. The LEF depends on the cavity losses because the laser resonance approaches the DOS maximum when the threshold gain increases. At still higher carrier densities, the LEF starts increasing again because of the gain saturation of the ground state. The envelope overlap function appearing in the optical matrix element influences the LEF through the same mechanisms as the cavity losses.

The LEF is not strongly temperature dependent near room temperature, but it begins to increase at low and high temperatures, the limits depending on the energy separation of the dot energy states.

B. Laser operation away from the gain maximum

Next, we assumed that the lasers were forced to operate 12 meV above the gain maximum of the previous section by using frequency selective cavities. The corresponding emission energies are $\hbar\omega^{\mathrm{QDL}}=1030\,\mathrm{meV}$ (this is 5 meV above the QDL ground state DOS maximum) and $\hbar\omega^{\mathrm{QWL}}=1022\,\mathrm{meV}$. As a result the refractive index of the QDL [Fig. 4(b)] changes drastically. The LEF of the QDL at this operation point reduces to LEF$\approx$0.04. For the QWL the LEF becomes $\sim$1.1. This energy shift also increases the threshold carrier density [Fig. 4(a)] and threshold current to $n_{\mathrm{th}}^{\mathrm{QDL}}=1.9\times10^{21}\,\mathrm{m}^{-3}$ (36% increase) and *QWL* $5.0\times10^{22}\,\mathrm{m}^{-3}$ (11% increase) for the QDL and the QWL, respectively.

It is concluded that, due to the shape of the DOS, the LEF of a QDL can be made approximately zero by blueshifting the operation point from the gain maximum. In the case of a QWL the value of the LEF does decrease but it is unlikely that the value zero can be obtained for realistic structures under lasing conditions.

C. Chirp

We have used the rate equations [Eqs. (8) and (9)] in their simplest form to calculate an estimate for the chirp of the two lasers. A 1 GHz sinusoidal signal biased at $I_{\mathrm{th}}+3.6\,\mathrm{mA}$ and amplitude $1.6\times3.6\,\mathrm{mA}$ was used as a stimulus in the rate equations for both lasers. The threshold currents were set to 4 and 30 mA for the QDL and QWL, respectively, and the spontaneous emission coupling η was given a value of 10^{-4}. When the two lasers were made to operate at the gain maximum, the changes of the refractive index were 1.5×10^{-4} (QDL) and 1.0×10^{-4} (QWL), and the resulting chirps became $\Delta\lambda\approx0.19\,\mathrm{nm}$ (37 GHz) and 0.13 nm (25 GHz). The modulation used to calculate the chirp pushed the lasers below the threshold, and therefore the values of the chirp are not in good proportion to the values of the LEF.

For the blueshifted lasers, the changes of refractive indices for the QDL and QWL became 6×10^{-6} and 5.4×10^{-5}, respectively. The corresponding chirps are $\Delta\lambda\approx0.0074\,\mathrm{nm}$ (1.5 GHz) and 0.067 nm (13 GHz). The very low LEF of the blueshifted QDL makes its frequency almost independent of the strong current modulation.

D. Comparison to experiments and other calculations

The laser structures used here are idealizations regarding the strict selection rules, perfect Gaussian inhomogeneous broadening of QD states, and single mode laser operation, etc. However, qualitatively our results agree well with the measured photon energy and carrier density dependence of the LEF.[6,20–22] Note that the record low LEF value 0.1 in Ref. 6 was obtained below the laser threshold.

Our first approximation calculations neglect quantitative treatment of transition amplitudes and nonlinearities in the absorption as well as band gap renormalization. Recently, Schneider *et al.*[13] treated the latter two effects using the semiconductor Bloch equation approach. They excluded the interactions of carriers confined in the QD's. However, according to recent first principles calculations of Braskén *et al.*[23] these interactions are very prominent. The most puzzling feature is that the experiment[24] does not agree with the reported large redshifts of Schneider *et al*. Therefore further theoretical and computational work is still needed to quantify our present understanding of QDL dynamics.

V. CONCLUSIONS

We have calculated the gain, refractive index, LEF, and chirp of a QDL and a QWL in the quasiequilibrium distribution and parabolic band approximations. We found that the dominant contribution to the LEF results from the QD ground state emission line itself. We also show in the Appendix that, in counterdistinction to a previous work,[12] even for a single isolated inhomogeneously broadened emission line the LEF is never zero at the gain maximum.

We found that the LEF can be made zero if the absorption spectrum of a QDL for a very low carrier density decreases strongly above (within $\sim kT$) the laser frequency. For a QDL with widely separated absorption peaks this requirement is well satisfied. The inhomogeneous broadening mainly determines the magnitude of the blueshift required to attain zero LEF: the smaller the broadening, the smaller the blueshift. Small detuning generally increases the threshold current of the laser by a few tens of percent.

APPENDIX

In this appendix we consider the LEF of a single isolated discrete resonance line. We account for the inhomogeneous broadening and assume thermal quasiequilibrium. There are two goals for this appendix. First, we study the small inho-

mogeneous broadening region ($\sigma \ll kT$) and show that the LEF evaluated at the gain maximum does not approach zero even at the limit of zero inhomogeneous broadening. Note that we retain the assumption that homogeneous broadening is insignificant in comparison to the inhomogeneous broadening. Second, we plot the LEF for various injection levels and emission energies.

We start by replacing the Fermi distribution of the conduction band electrons by the linear approximation

$$f_c(E) = \frac{1}{2} - \frac{E - E_f^c}{4kT}, \tag{A1}$$

where E_f^c is the Fermi energy of the electrons. This approximation is good when $(E - E_f^c) \ll kT$.

When we assume that the densities of electrons and holes in the system are equal and replace the Fermi modulation $f_c - f_v$ of Eq. (4) with $2f_c(E) - 1$, the gain of the ensemble in the linear approximation is given by

$$G(\hbar\omega, E_f^c) = \frac{G_{\max}\sigma_0}{4\sigma kT} e^{-(\hbar\omega - E_0)^2/2\sigma^2} (\hbar\omega - E_0 - 2E_f^c). \tag{A2}$$

Here E_0 is the energy of the Gaussian resonance line. To keep the total number of electron states constant while changing the inhomogeneous broadening σ, we have normalized the maximum gain as $G_{\max}\sigma_0/\sigma$. Here $G_{\max}$ is the maximum gain occurring at complete inversion ($E_f^c = \infty$) for inhomogeneous broadening $\sigma = \sigma_0$. The transition energy $\hbar\omega$ and electron energy E are related by $E = (\hbar\omega - E_0/2)$. The energy zero is set to the maximum of the conduction band DOS.

The location of the gain maximum is found by maximizing Eq. (A2) with respect to $\hbar\omega$ and is given by

$$\hbar\omega_G = E_0 + E_f^c - \sqrt{(E_f^c)^2 + \sigma^2}. \tag{A3}$$

The Fermi level at laser threshold is now obtained from Eq. (A2) by solving $G(\hbar\omega_G, E_f^c) = \alpha$ for E_f^c:

$$E_f^c = \frac{\sigma\sqrt{2}}{2}\left[1 - L_\omega\left(\frac{G_{\max}^2\sigma_0^2}{16\alpha^2k^2T^2}\right)\right] \Bigg/ \sqrt{L_\omega\left(\frac{G_{\max}^2\sigma_0^2}{16\alpha^2k^2T^2}\right)}$$

$$= C_L\sigma. \tag{A4}$$

Here L_ω is the Lambert W function satisfying $L_\omega(x)\exp[L_\omega(x)] = x$, and α is the total loss of the laser cavity. Note that in this approximation the Fermi level is linearly dependent on σ. Therefore the condition $\sigma \ll kT$ leads to $(E - E_f^c) \ll kT$ for $\alpha \ll G_{\max}\sigma_0/\sigma$ and the linear Fermi approximation is justified.

The LEF can also be defined using the Fermi levels as

$$\mathrm{LEF} = -k_0 \frac{\partial n_r / \partial E_f^c}{\partial G / \partial E_f^c}. \tag{A5}$$

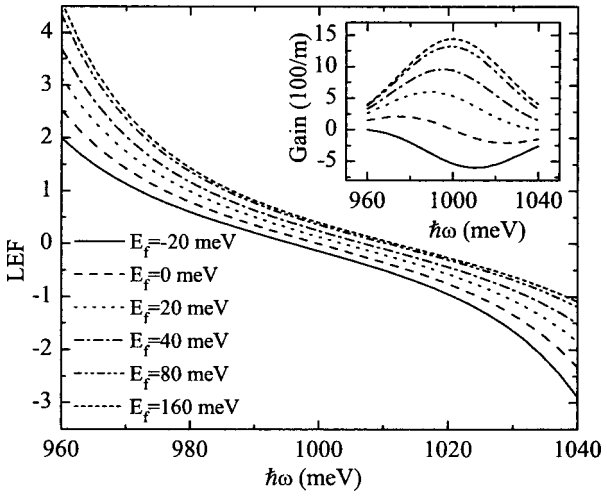

FIG. 5. The contribution of an inhomogeneously broadened isolated ground state to LEF as a function of transition energy for different injection levels (the Fermi levels E_f^c are measured from the center of the conduction band ground state). The inset shows the corresponding gain profiles. We notice that the ground state LEF is not generally zero.

Next we substitute the gain [Eq. (A2)] and the refractive index [Eq. (6)] in Eq. (A5) and move the derivative inside the integral of Eq. (6). We also divide the integrand into symmetric and antisymmetric functions with respect to $\hbar\omega$. Here we assume for simplicity that the factor $1/(E^2 - \hbar^2\omega^2)$ is antisymmetric with respect to $\hbar\omega$, which is an acceptable approximation for the energies concerned. Eliminating the antisymmetric integral gives

$$\mathrm{LEF} = \int_0^{\hbar\omega} -4ch e^{-(\hbar\omega - E)^2/2\sigma^2}$$

$$= \times \frac{\sinh[(\hbar\omega - E)(\hbar\omega - E_0)/\sigma^2]}{\pi\lambda(\hbar\omega - E)(\hbar\omega + E)} dE. \tag{A6}$$

Making the change of variables $E \to \sqrt{2}\sigma u + \hbar\omega$ and substituting $\hbar\omega_G$ [Eq. (A3)] and E_f^c [Eq. (A4)] gives in the limit $\sigma \to 0$

$$\mathrm{LEF} = \frac{-4ch}{\pi\lambda} \int_{-\hbar\omega_G/\sqrt{2}\sigma}^{0} \frac{e^{-u^2}\sinh(\sqrt{2}uC)}{u(2\hbar\omega_G + \sqrt{2}\sigma u)} du$$

$$\to \frac{-4ch}{\pi\lambda a\hbar\omega_G} \int_{-\infty}^{0} \frac{e^{-u^2}\sinh(\sqrt{2}uC)}{u} du$$

$$= \frac{-2ch}{\lambda a\hbar\omega_G} \mathrm{erfi}\left(\frac{\sqrt{2}}{2}C\right). \tag{A7}$$

The factor $2\hbar\omega_G + \sigma E$ has been replaced with $a\hbar\omega_G$, where $a \subseteq [1, 2]$ and $C = C_L - \sqrt{C_L^2 + 1}$ [see Eq. (A4)]. Equation (A7) gives the upper and lower bounds to the value of the LEF. At the small σ limit $a \approx 2$, because the integrand is peaked close to $\sigma u = 0$. For QDL parameters like those used for ES1, the lower bound is ≈ 1.

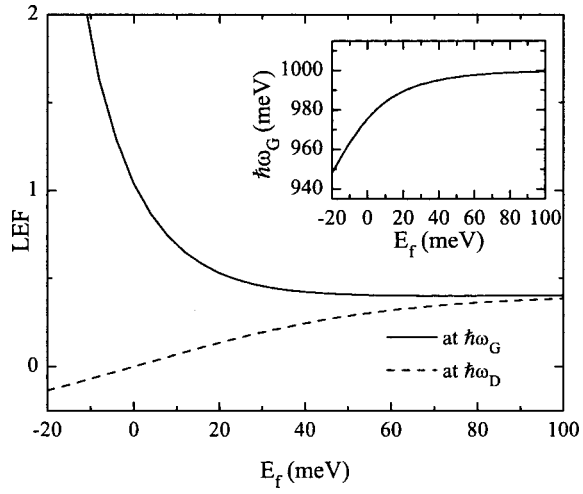

FIG. 6. The contribution of an inhomogeneously broadened isolated ground state to LEF as a function of the Fermi level. The LEF is calculated for two different energies: for the energy of DOS maximum $\hbar\omega_D\,(=E_0)$ and for the energy at which the gain maximum occurs $\hbar\omega_G$. The location of the gain maximum $\hbar\omega_G$ is plotted in the inset as a function of the injection level.

For comparison, we also calculated the LEF of an inhomogeneously broadened isolated ground state *without* incorporating the linear Fermi approximation but assuming the antisymmetry of the factor $1/(E^2-\hbar\omega_G^2)$. The parameters of the ensemble were chosen to be $\sigma=25$ meV and $E_0=1$ eV. The results are shown in Figs. 5 and 6. Note that the LEF of a laser operating at the gain maximum approaches the value of LEF of a laser operating at the DOS maximum at high injection levels. In real structures, however, the gain saturation in the presence of excited states starts to increase the LEF significantly at high carrier densities. We conclude that for inhomogeneously broadened quasithermally distributed quantum dots the ground state contribution to the LEF is never zero when the laser operates at the gain maximum, contrary to Ref. 12.

[1] P. Borri, W. Langbein, J. M. Hvam, F. Heinrichsdorff, M.-H. Mao, and D. Bimberg, IEEE J. Sel. Top. Quantum Electron. **6**, 544 (2000).
[2] K. Kim, J. Urayama, and T. B. Norris, Appl. Phys. Lett. **81**, 670 (2002).
[3] M. Braskén, M. Lindberg, M. Sopanen, H. Lipsanen, and J. Tulkki, Phys. Rev. B **58**, R15 993 (1998).
[4] H. Saito, K. Nishi, A. Kamei, and S. Sugou, IEEE Photonics Technol. Lett. **12**, 1298 (2000).
[5] G. Park, O. Shchekin, D. Huffaker, and D. Deppe, IEEE Photonics Technol. Lett. **13**, 230 (2000).
[6] T. Newell, D. Bossert, A. Stintz, B. Fuchs, K. Malloy, and L. Lester, IEEE Photonics Technol. Lett. **11**, 1527 (1999).
[7] D. Huffaker and D. Deppe, Appl. Phys. Lett. **73**, 520 (1998).
[8] Y. Arakawa and H. Sakaki, Appl. Phys. Lett. **40**, 939 (1982).
[9] M. Asada, Y. Miyamoto, and Y. Suematsu, IEEE J. Quantum Electron. **22**, 1915 (1986).
[10] K. J. Vahala, IEEE J. Quantum Electron. **24**, 523 (1988).
[11] M. Grundmann and D. Bimberg, Jpn. J. Appl. Phys., Part 1 **36**, 4181 (1997).
[12] D. Bimberg, N. Kirstaedter, N. N. Ledentsov, Z. I. Alferov, P. S. Kop'ev, and V. M. Ustinov, IEEE J. Sel. Top. Quantum Electron. **3**, 196 (1997).
[13] H. C. Schneider, W. W. Chow, and S. W. Koch, Phys. Rev. B **66**, 041310 (2002).
[14] M. Asada, IEEE J. Quantum Electron. **25**, 2019 (1989).
[15] M. Yamada, S. Ogita, M. Yamagishi, and K. Tabata, IEEE J. Quantum Electron. **21**, 640 (1985).
[16] P. Bhattacharya, Semiconductor Optoelectronic Devices, 2nd ed. (Prentice-Hall, Englewood Clifts, NJ, 1997).
[17] L. Asryan, M. Grundmann, N. Ledentsov, O. Stier, R. Suris, and D. Bimberg, J. Appl. Phys. **90**, 1666 (2001).
[18] A. Heinämäki and J. Tulkki, J. Appl. Phys. **81**, 3268 (1997).
[19] L. Lester, A. Stintz, H. Li, T. Newell, E. Pease, B. Fuchs, and K. Malloy, IEEE Photonics Technol. Lett. **11**, 931 (1999).
[20] M.-H. Mao, F. Heinrichsdorff, and D. Bimberg, in 11th International Conference on Indium Phosphide and Related Materials (Davos, Switzerland, 1999), pp. 569–571.
[21] Y. Huang, S. Arai, and K. Komori, IEEE Photonics Technol. Lett. **5**, 142 (1993).
[22] L. D. Westbrook and M. J. Adams, Proc. IEEE **135**, 223 (1988).
[23] M. Braskén, M. Lindberg, D. Sundholm, and J. Olsen, Phys. Rev. B **61**, 7652 (2000).
[24] H. Lipsanen, M. Sopanen, and J. Ahopelto, Phys. Rev. B **51**, 13 868 (1995); similar results have been obtained for InGaAs/GaAs pyramid structures.